Node-Localized Transporters of Phosphorus Essential for Seed Development in Rice

Jing Che [ID] [1], Naoki Yamaji[1], Takaaki Miyaji[2], Namiki Mitani-Ueno[1], Yuri Kato[2], Ren Fang Shen[3] and Jian Feng Ma [ID] [1,*]

[1]Institute of Plant Science and Resources, Okayama University, Chuo 2-20-1, Kurashiki, 710-0046 Japan
[2]Advanced Science Research Center, Okayama University, Okayama, 700-8530 Japan
[3]State Key Laboratory of Soil and Sustainable Agriculture, Institute of Soil Science, Chinese Academy of Sciences, Nanjing 210008, China
*Corresponding author: E-mail, maj@rib.okayama-u.ac.jp, Fax, +81-86-434-1209.

About 60–85% of total phosphorus (P) in cereal crops is finally allocated to seeds, where it is required for seed development, germination and early growth. However, little is known about the molecular mechanisms underlying P allocation to seeds. Here, we found that two members (*OsPHO1;1* and *OsPHO1;2*) of the *PHO1* gene family are involved in the distribution of P to seeds in rice. Both OsPHO1;1 and OsPHO1;2 were localized to the plasma membrane and showed influx transport activities for inorganic phosphate. At the reproductive stage, both *OsPHO1;1* and *OsPHO1;2* showed higher expression in node I, the uppermost node connecting to the panicle. *OsPHO1;1* was mainly localized at the phloem region of diffuse vascular bundles (DVBs) of node I, while *OsPHO1;2* was expressed in the xylem parenchyma cells of the enlarged vascular bundles (EVBs). In addition, they were also expressed in the ovular vascular trace, the outer layer of the inner integument (*OsPHO1;1*) and in the nucellar epidermis (*OsPHO1;2*) of caryopses. Knockout of *OsPHO1;2*, as well as *OsPHO1;1* to a lesser extent, decreased the distribution of P to the seed, resulting in decreased seed size and delayed germination. Taken together, *OsPHO1;2* expressed in node I is responsible for the unloading of P from the xylem of EVBs, while *OsPHO1;1* is involved in reloading P into the phloem of DVBs for subsequent allocation of P to seeds. Furthermore, *OsPHO1;1* and *OsPHO1;2* expression in the caryopsis is important for delivering P from the maternal tissues to the filial tissues for seed development.

Keywords: Caryopsis • Influx transporter • Node • Phloem • Phosphorus • Seed development.

Introduction

In cereal crops, such as rice (*Oryza sativa*), about 60–85% of aboveground phosphorus (P) is finally allocated to seeds and stored mainly in the form of phytate (Raboy 2001, Lott et al. 2009). Phytate in seeds has both beneficial and negative effects. Proper accumulation of phytate is required for seed development, seed germination and early growth (White and Veneklaas 2012). It was reported that a seed P concentration higher than $1\,mg\,g^{-1}$ is required for this function (Pariasca-Tanaka et al. 2015). However, a high accumulation of phytate causes environmental and nutritional problems. This is because phytate cannot be digested by humans and monogastric animals, and almost 90% of phytate in animal feed is thus excreted into rivers, lakes and oceans, causing eutrophication. Furthermore, phytic acid forms strong complexes with metals, such as zinc and iron, thereby inhibiting theuptake of these elements by the gut (Raboy 2001, 2009).Therefore, it is important to balance P accumulation in theseeds for crop productivity, the environment and human nutrition.

There are two sources of P in rice seeds:re-translocation from old leaves and distribution of P newly taken up after the flowering stage (Yamaji et al. 2017, Chang et al. 2019). The latter is mediated by various transporters localized in the nodes, especially in node I, the uppermost node connecting to the panicles. Rice nodes have highly developed vascular systems, mainly consisting of enlarged vascular bundles (EVBs) and diffuse vascular bundles (DVBs) (Yamaji and Ma 2014, 2017). EVBs come from the two lower nodes and are connected to the leaf attached to the node, while DVBs start at the node and are connected to the upper two nodes or panicle (Yamaji and Ma 2014). Therefore, after an element is taken up by the root and translocated to node I, an intervascular transfer of mineral elements from EVBs to DVBs is required for its distribution to the seeds. A few transporters involved in the intervascular transfer of mineral elements have been identified. For example, the distribution of(Si) to the seeds is mediated by three different Si transporters, Lsi6, Lsi2 and Lsi3, in rice. They are localized at xylem parenchyma cells, bundle sheath cells of EVBs, and in parenchyma bridge cells between EVBs and DVBs, respectively, and are responsible for the transfer of Si from the xylem of EVBs to the xylem of DVBs (Yamaji et al. 2008, Yamaji and Ma 2009, Yamaji et al. 2015). On the other hand, two transporters, OsZIP3 and OsHMA2, are involved in the distribution of (Zn) to seeds in rice (Yamaji et al. 2013b, Sasaki et al. 2015). OsZIP3 is localized at the xylem transfer cells in EVBs and is involved in the unloading of Zn from the xylem of EVBs (Sasaki et al. 2015),

while OsHMA2 is localized at the phloem region of both EVBs and DVBs and is responsible for loading Zn to the phloem of DVBs and EVBs (Yamaji et al. 2013b). Recently, a novel P transporter, SPDT, was reported to be responsible for the distribution of P to seeds in rice (Yamaji et al. 2017). SPDT is localized at the xylem parenchyma cells of nodes and mediates transient incorporation of P from the xylem to the nodal tissues, which promotes P transfer from the xylem to the phloem and also from EVBs to DVBs in the node (Yamaji et al. 2017). However, most transporters involved in the distribution of mineral elements, including P, in the nodes have not been identified. Our previous RNA-seq analysis of node I revealed that two genes (*OsPHO1;1* and *OsPHO1;2*) belonging to the PHOSPHATE1 (PHO1) gene family showed very high expression (Yamaji et al. 2013a).

PHO1 was first identified in Arabidopsis (Hamburger et al. 2002). It is primarily expressed in the root vascular cylinder. A knockout of this gene resulted in decreased P concentration in the shoots but increased P in the roots (Poirier et al. 1991), indicating its involvement in P transfer from roots to shoots in Arabidopsis. There are three homologs of Arabidopsis *PHO1* in the rice genome, *OsPHO1;1*, *OsPHO1;2* and *OsPHO1;3*, with 46–68% identity (Secco et al. 2010). However, only the knockout of *OsPHO1;2* but not of *OsPHO1;1* showed a similar phenotype as the Arabidopsis *pho1* mutant (Secco et al. 2010). *OsPHO1;2* is also expressed in the xylem parenchyma cells of rice roots (Jabnoune et al. 2013), indicating that, similar to Arabidopsis PHO1, OsPHO1;2 also plays an important role in the root-to-shoot translocation of P in rice. Functional analysis of SlPHO1;1 in tomato also revealed its role in the root-to-shoot translocation of P at the seedling stage (Zhao et al. 2019). In the present study, we focus on the role of *OsPHO1;1* and *OsPHO1;2* expressed in node I in P distribution to seeds at the reproductive growth stage. We found that *OsPHO1;1* and *OsPHO1;2* are expressed in different tissues of node I and in caryopses, and that they are involved in the allocation of P to the seeds.

Results

Expression patterns of *OsPHO1;1* and *OsPHO1;2*

According to our RNA-seq data of rice node I (Yamaji et al. 2013a), among three *PHO1* genes in rice, *OsPHO1;1* and *OsPHO1;2*, but not *OsPHO1;3*, showed higher expression in this organ. We therefore investigated the expression pattern of *OsPHO1;1* and *OsPHO1;2* in different organs at the grain-filling stage of rice grown in the field. *OsPHO1;1* was mainly and highly expressed in node I (**Fig. 1A**). *OsPHO1;2* was also highly expressed in node I (**Fig. 1B**). In addition, its expression was found in roots and in shoot basal stems, including the basal node (**Fig. 1B**).

To examine the tissue specificity of *OsPHO1;1* and *OsPHO1;2* expression in node I, we separated node I into different tissues by using laser microdissection (LMD). Consequently, we found that *OsPHO1;1* was mainly expressed in the DVBs of node I (**Fig. 1C**). By contrast, *OsPHO1;2* was highly expressed in the xylem regions of EVBs in node I (**Fig. 1D**).

Subcellular localization of OsPHO1;1 and OsPHO1;2

To determine the subcellular localization of OsPHO1;1 and OsPHO1;2, the open reading frame (ORF) of *OsPHO1;1* and *OsPHO1;2* was fused with green fluorescence protein (GFP) at the C-terminus and N-terminus, respectively. The fused genes were introduced into the rice leaf protoplast under the control of a 35S promoter. The GFP signal in the cells expressing the fusion genes was detected at the cell periphery outward from the chloroplast (**Supplementary Fig. S1E–L**). By contrast, the GFP signal was detected in the cytosol and nucleus in rice protoplasts expressing GFP alone (**Supplementary Fig. S1A–D**). These results indicate that both OsPHO1;1 and OsPHO1;2 are localized to the plasma membrane.

Tissue specificity and cell specificity of *OsPHO1;1* and *OsPHO1;2* expression in node I and caryopsis

To investigate the tissue- and cell-specific expression of *OsPHO1;1* and *OsPHO1;2*, we generated transgenic rice lines carrying GFP fused with the *OsPHO1;1* or *OsPHO1;2* promoter (*OsPHO1;1_{pro}-GFP* and *OsPHO1;2_{pro}-GFP*) and performed immunostaining with a GFP antibody. In node I, a strong signal in plants carrying *OsPHO1;1_{pro}-GFP* was detected in the phloem region of the DVBs (**Fig. 2A, B**). Some weak signal was also detected in the phloem region of the EVBs (**Fig. 2A, B**). By contrast, GFP signal in plants carrying *OsPHO1;2_{pro}-GFP* was observed in the xylem parenchyma cells including transfer cells of the EVBs in node I (**Fig. 2C, D**). These results are consistent with the expression pattern in different tissues of node I by LMD (**Fig. 1C, D**). No signal was observed in node I in non-transgenic wild-type (WT) rice (**Fig. 2E**), indicating the specificity of the antibody.

Occasionally, we also found that both *OsPHO1;1_{pro}-GFP* and *OsPHO1;2_{pro}-GFP* were expressed in the ovular vascular trace (OVT) of caryopses at day 6 after pollination (**Fig. 3A, B, D and E**). Furthermore, in contrast to *OsPHO1;1*, which was expressed in the outer layer of the inner integument (**Fig. 3A–C**), *OsPHO1;2* was expressed in the nucellar epidermis of the caryopsis (**Fig. 3D–F**). No signal was observed in the caryopsis of WT (**Fig. 3G**).

Phenotypic analysis of *ospho1;1* and *ospho1;2* mutants grown in paddy fields

To investigate the physiological role of *OsPHO1;1* and *OsPHO1;2* in rice, we obtained two independent *Tos17* retrotransposon insertion lines for each gene (**Supplementary Fig. S2A, B**). Reverse transcription PCR analysis showed that no transcript of *OsPHO1;1* or *OsPHO1;2* was detected in the *ospho1;1* and *ospho1;2* mutants, respectively (**Supplementary Fig. S2C**), indicating that they are knockout lines.

Some agronomic traits were compared at harvest between mutant and WT rice plants grown in a paddy field. Plant height and panicle number were lower in both *ospho1;1* and *ospho1;2* mutants compared with WT (**Fig. 4A, B**). However, the grain number per panicle and the percentage of filled spikelets were similar between the two mutants and the WT, although *ospho1;1* mutant and *ospho1;2* mutant showed lower grain number per
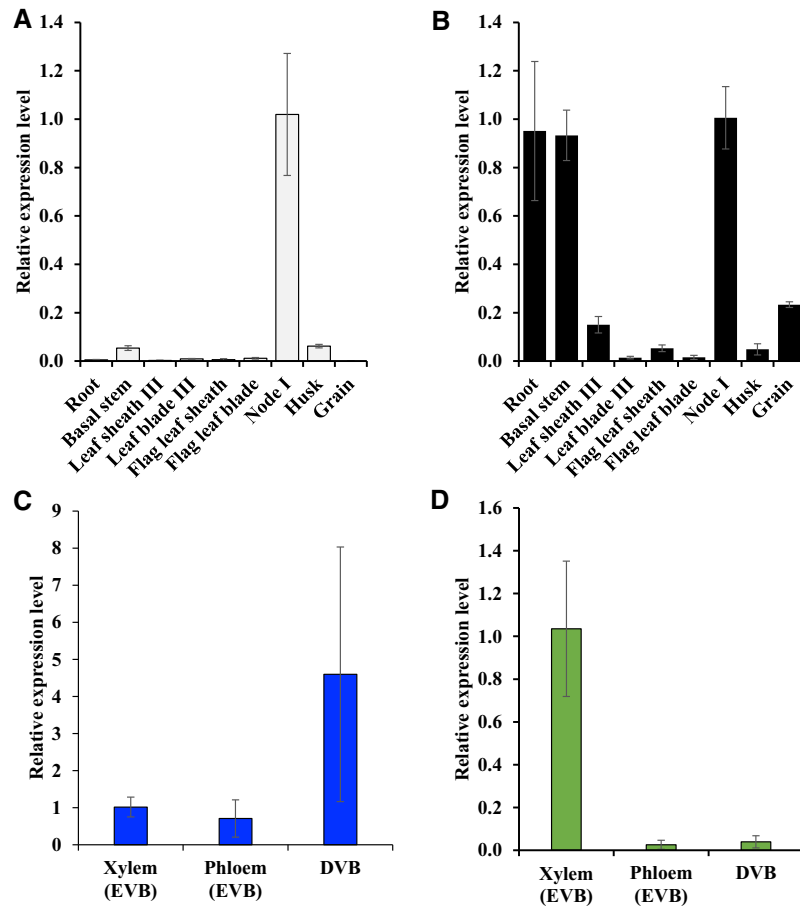
Fig. 1 Expression pattern of *OsPHO1:1* and *OsPHO1;2* at the reproductive growth stage. Relative expression level of *OsPHO1;1* (A) and *OsPHO1;2* (B) in various organs. Rice was grown in a paddy field, and various organs were sampled at the grain-filling stage. Tissue specificity of the expression of *OsPHO1;1* (C) and *OsPHO1;2* (D) in node I. Node I sampled at the milky stage was separated into different tissues by laser microdissection. The expression level was determined by quantitative RT-PCR. Expression relative to node I (A and B), to the xylem (EVB) (C and D) is shown. *HistoneH3* and *Actin* were used as internal standards in (A) and (B), and (C) and (D), respectively. Data are means ± SD of three biological replicates.

panicle (**Fig. 4C, D**). The most obvious difference between WT and mutants was found when comparing grain size (**Fig. 4E, F**). The 1,000-grain weight of the *ospho1;2* mutants was only 52–58% that of WT (**Fig. 4E**), although it was almost unchanged in *ospho1;1* mutants (**Fig. 4E**). As a result, the grain yield was reduced by 17–18% in the *ospho1;1* mutants but only by 54–65% in the *ospho1;2* mutants (**Fig. 4F**). Moreover, the grain of *ospho1;2* mutants was shriveled while that of *ospho1;1* mutants was similar to WT (**Fig. 4G**).

Knockout of *OsPHO1;1* and *OsPHO1;2* resulted in decreased P allocation to seeds

The profile of mineral elements was compared in different organs at harvest between WT and the knockout lines grown in a paddy field. Among the mineral elements examined, only P showed a consistent difference between WT and mutants in different organs. Compared with WT, *ospho1;1* mutants accumulated higher P in leaf II sheath, internode II, brown rice and in remaining straw parts (**Fig. 5A**). In *ospho1;2* mutant lines, the P concentration in node II, node I, and husk was significantly higher than in WT, but it was decreased in leaf II blade, flag leaf blade and brown rice compared with WT (**Fig. 5B**). Notably, the P concentration in brown rice was 44–50% lower in the *ospho1;2* mutant than in the WT (**Fig. 5B**). The concentration of other elements, including K, Mg, Fe, Mn and Zn, was similar in each organ between mutants of *ospho1;1* and *ospho1;2*, and WT except that *ospho1;2* mutants accumulated lower K in the peduncle and higher Mg in most organs (**Supplementary Fig. S3**).

Distribution ratio of P to different organs was calculated and compared between mutants and WT. In *ospho1;1* mutants, less P was delivered to brown rice, but more P was distributed to internode II, leaf sheath of leaf II and remaining straw parts compared with WT (**Fig. 5C**). In *ospho1;2* mutants, much less P was delivered to brown rice, whereas more P was delivered to the leaf II sheath, internode II, husk and remaining straw parts compared with WT (**Fig. 5D**).

Short-term stem-feeding experiment with radioisotope [32]P

Since the knockout of *OsPHO1;1* and *OsPHO1;2* affected growth (**Fig. 4F**), there is a possibility that the differences in P
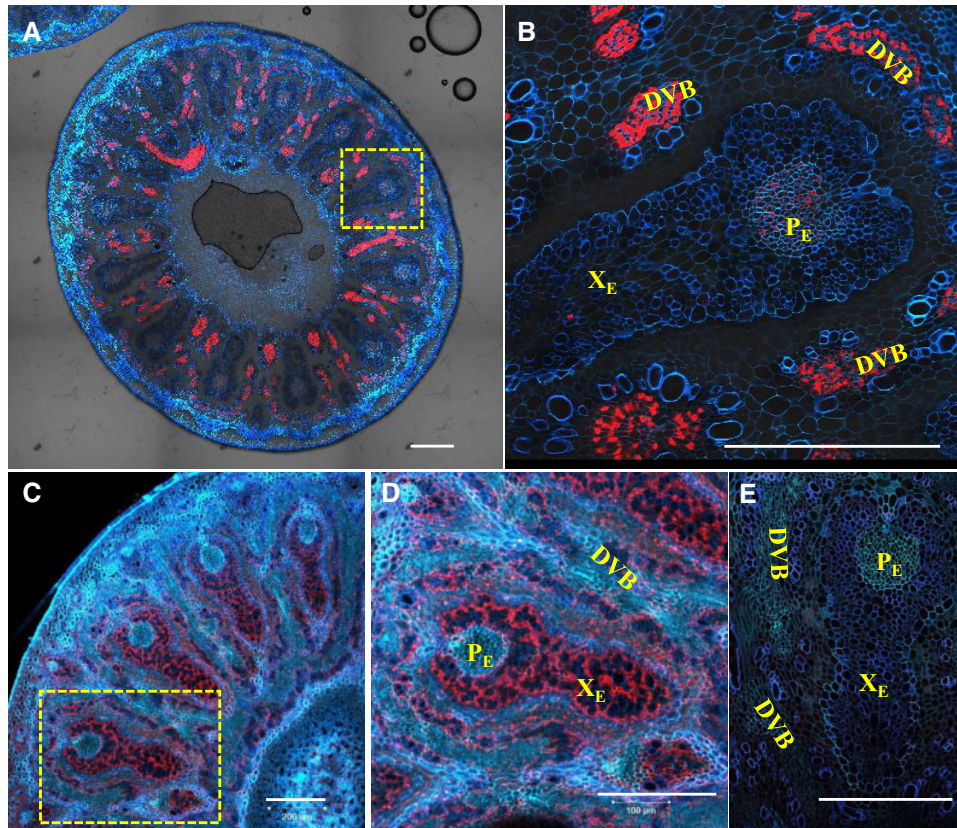
Fig. 2 Tissue specificity and cell specificity of *OsPHO1;1* and *OsPHO1;2* expression in node I. Immunostaining with a GFP antibody was performed in transgenic rice carrying the *OsPHO1;1* (A and B) or *OsPHO1;2* (C and D) promoter fused with GFP or WT rice (E) as a negative control. Red color indicates the GFP antibody-specific signal. Blue color indicates cell wall autofluorescence. Yellow dotted boxes in (A) and (C) represent regions magnified in (B) and (D), respectively. The xylem area of enlarged vascular bundle (X_E), DVBs and phloem area of enlarged vascular bundle (P_E) in the node I are shown. Node I was sampled from rice grown in soil at the grain-filling stage. Scale bars, 200 μm.
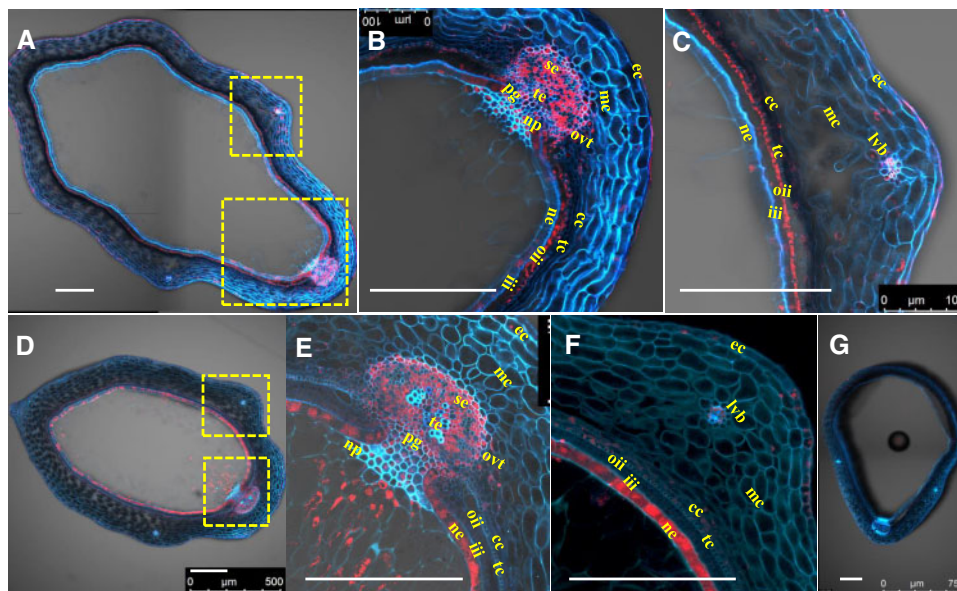

Fig. 3 Expression of *OsPHO1;1* and *OsPHO1;2* in the caryopsis. Immunostaining with a GFP antibody was performed in transgenic rice carrying the *OsPHO1;1* (A–C) or *OsPHO1;2* (D–F) promoter fused with GFP or WT rice (G) as a negative control. Red color indicates the GFP antibody-specific signal. Blue color indicates cell wall autofluorescence. Yellow dotted boxes in (A) and (D) represent regions magnified in (B) and (C) and (E) and (F), respectively. The caryopsis was prepared from the dehusked grain at day 6 after pollination. Scale bars, 200 μm. ec, epicarp; mc, mesocarp; np, nucellar projection; cc, cross cell; tc, tube cell; oii, outer layer of inner integument; iii, inner layer of inner integument; ne, nucellar epidermis, te, tracheary elements; se, sieve elements; lvb, lateral vascular bundle; pg, pigment strand.
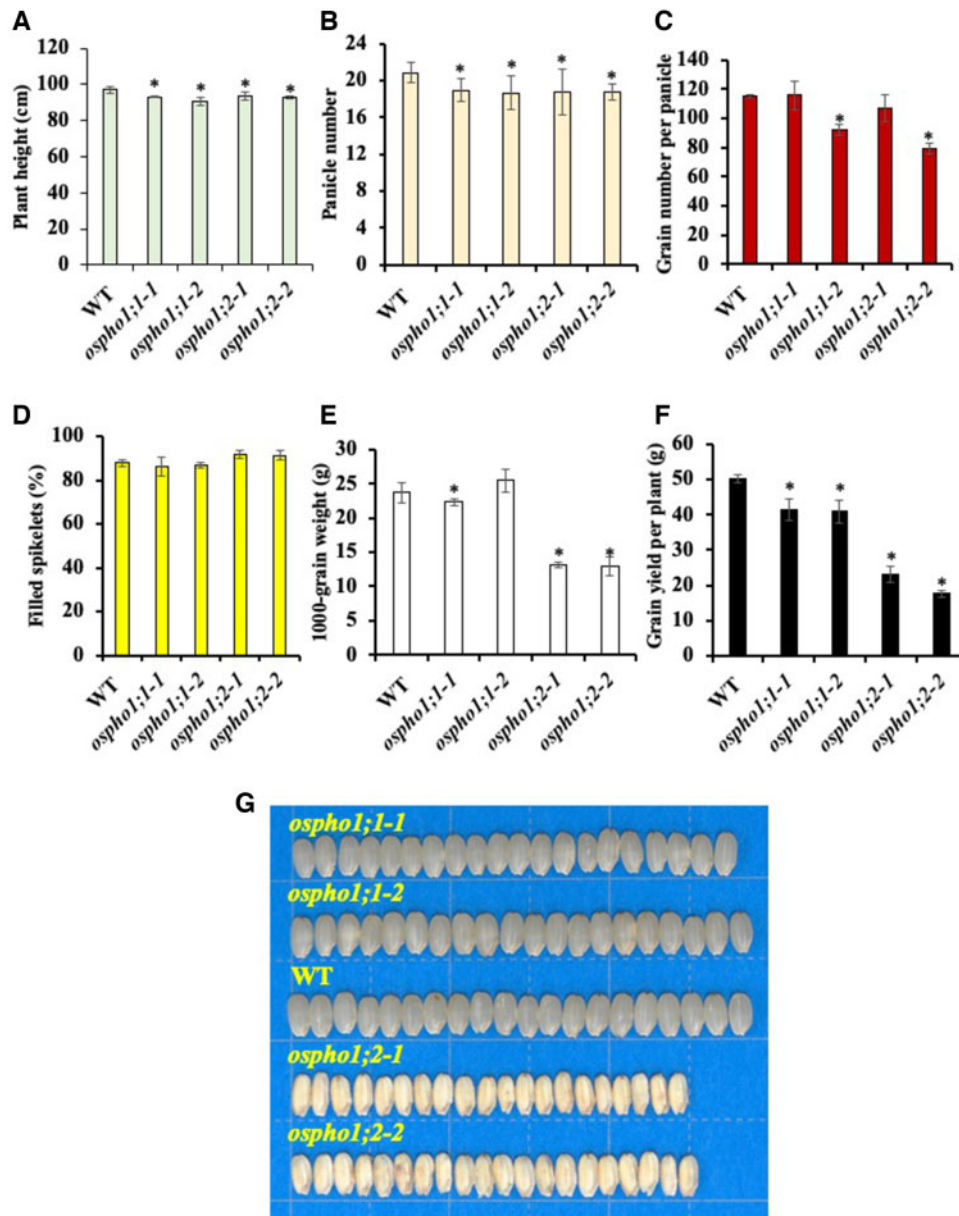
Fig. 4 Phenotypic analysis of *ospho1;1* and *ospho1;2* mutants. *ospho1;1*, *ospho1;2* mutant and WT rice plants were grown in a paddy field until maturing. At harvest, plant height (A), panicle number (B), grain number per panicle (C), percentage of filled spikelets (D), 1,000-grain weight (E) and grain yield (F) were measured and recorded. (G) Brown rice of WT, *ospho1;1* and *ospho1;2* mutant plants. Data are mean ± SD of 24 biological replicates (three plots with eight replicates each). $P < 0.05$, mutants compared with WT rice (Duncan's test).

distribution was indirectly caused by retarded growth. Furthermore, *OsPHO1;2* is involved in root-to-shoot translocation (Secco et al. 2010), which may also ultimately affect the distribution. To exclude these possibilities, we therefore performed a short-term (24 h) stem-feeding experiment with radioisotope ^{32}P. ^{32}P was fed from the cut end at internode III (below node II), and its distribution to different organs was compared in mutants and WT. As a result, distribution of ^{32}P to the panicle was decreased in the *ospho1;1* and *ospho1;2* mutants compared with the WT (Fig. 6), whereas that to the flag leaf was increased in the *ospho1;2* mutants.

Germination and early growth of *ospho1;1* and *ospho1;2* mutants

Since P concentration in the seeds was lower in *ospho1;2* mutants (Fig. 5B), we investigated whether this decrease affected seed germination and early growth of the seedlings. A time-course experiment up to 7 d showed that the germination of *ospho1;2* seeds was much slower than that of WT (Fig. 7A), but there was no difference in germination speed between WT and *ospho1;1* mutants (Fig. 7A). At 7 day, all lines reached a similar germination rate (Fig. 7A). The root growth of *ospho1;2* seedlings was also slower than that of WT (Fig. 7B),
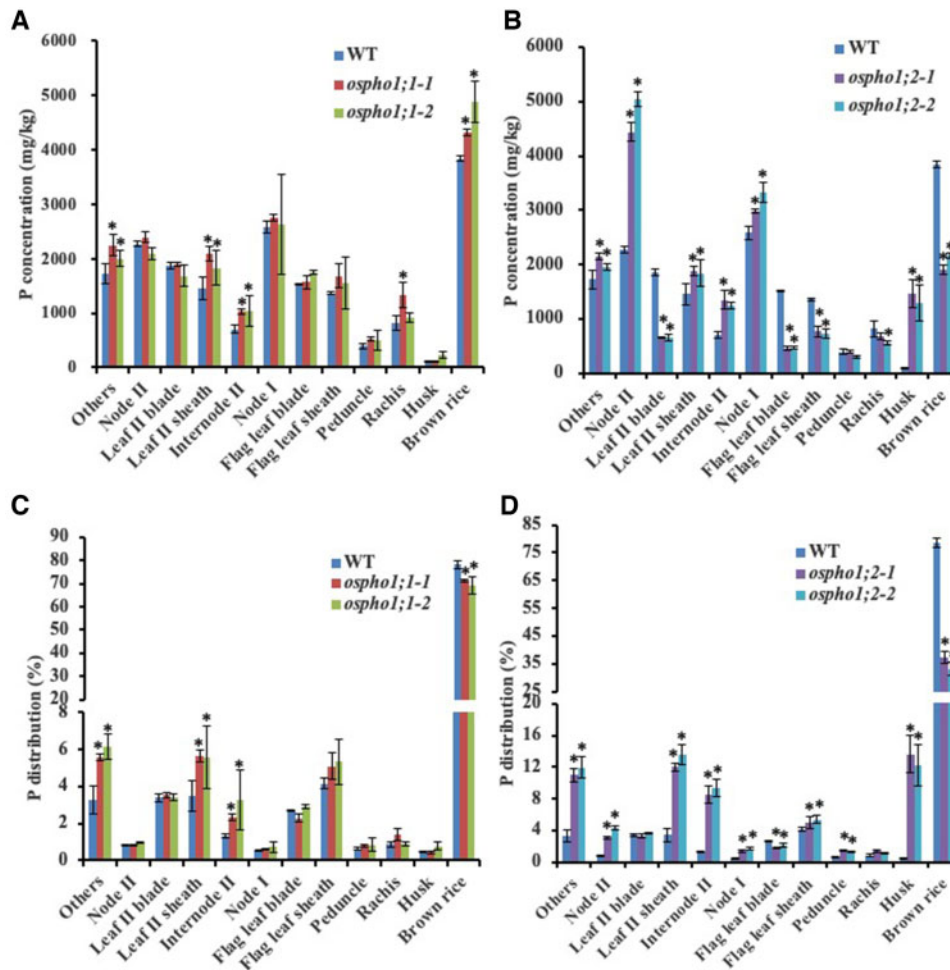
Fig. 5 Concentration and distribution of P at the reproductive growth stage. WT rice, *ospho1;1* and *ospho1;2* mutants were grown in a paddy field until ripening. (A and B) P concentration in different organs of the aboveground part. (C and D) P distribution ratio in different organs of the aboveground part. P distribution to different organs was calculated as P content in each organ/total P content × 100. Data are means ± SD of three biological replicates. Statistical comparison was performed by a one-way analysis of variance followed by Tukey's multiple comparison test. All data were compared with the WT ($P < 0.05$).

while root length of *ospho1:2* mutants was only 57–60% of the WT (**Fig. 7B, C**). However, there was no difference in root growth between WT and *ospho1;1* mutants (**Fig. 7B, C**). These results indicate that low P in the *ospho1;2* mutants affected both germination speed and early root growth.

Transport activity of OsPHO1;1 and OsPHO1;2

Since knockout of *OsPHO1;1* and *OsPHO1;2* specifically altered P distribution to seeds (**Fig. 5C, D**), we examined the transport activity of these two proteins for inorganic phosphate (Pi) both in a proteoliposome assay system and *Xenopus* oocytes. In the proteoliposome assay system, the cDNA of *OsPHO1;1* or *OsPHO1;2* was expressed in *Escherichia coli*. The purified protein fraction exhibited a major protein band with the expected apparent molecular mass of OsPHO1;1 and OsPHO1;2, being 110 kDa including YbeL (β) tag, which contains 121 amino acids (**Fig. 8A, Supplementary Fig. S4A**). This tag is necessary for expressing functional proteins in *E. coli*. In the proteoliposome assay system, the direction of purified protein was randomly

inserted in the liposome, but by changing the pH inside and outside of the liposome, this system allows us to determine both influx and efflux transport activities. For the determination of influx transport activity assay, the external pH was set to be lower than the internal pH (pH 5.6 vs. pH 7.0). No transport activity for radioisotope-labeled Pi was found when OsPHO1;2 was not included (**Fig. 8B**). However, the proteoliposomes containing the purified protein fraction of OsPHO1;1 or OsPHO1;2 as the sole protein source showed an H$^+$-dependent uptake activity for radioisotope-labeled Pi (**Fig. 8B, Supplementary Fig. S4B**). In the presence of carbonyl cyanide m-chlorophenylhydrazone (CCCP), a proton ionophore, the Pi transport activity of OsPHO1;1 and OsPHO1;2 was almost abolished (**Fig. 8B, Supplementary Fig. S4B**). Furthermore, the addition of 5 mM cold Pi significantly decreased Pi uptake (**Fig. 8B**). On the other hand, for the efflux transport activity assay, the external pH was set to be higher than the internal pH (pH 7.5 vs. pH 6.0). In contrast to influx transport activity, neither OsPHO1;1 nor OsPHO1;2 showed efflux transport activity for
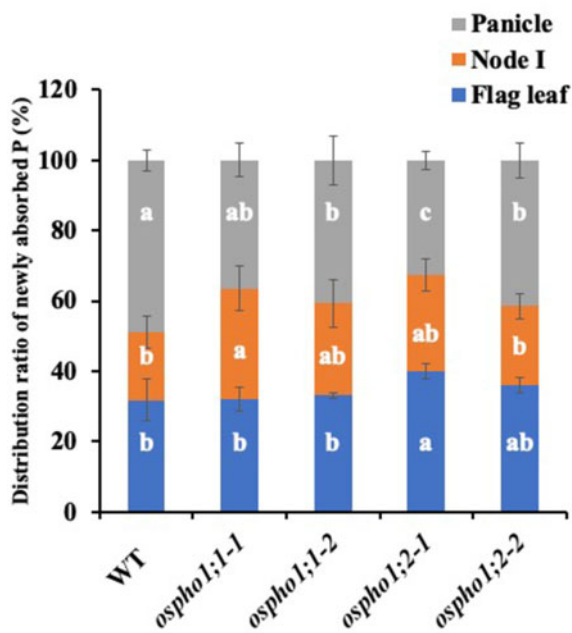
Fig. 6 Distribution of ^{32}P in different organs examined by short-term stem feeding. At the filling stage, WT, ospho1;1 and ospho1;2 mutant rice plants were cut at internode III. Solution containing 1 μM radioisotope-labeled Pi was fed from the cut-end of the stem for 24 h. The distribution ratio of newly absorbed P in different organs above node I was calculated. Data represent the mean ± SD ($n = 4$). Different lowercase letters indicate a significant difference between WT and mutants in the same tissues ($P < 0.05$) using Duncan's test.

Fig. 7 Seed germination and early growth of the seedlings. Germination rate (A) and root growth (B, C) of WT rice, ospho1;1 and ospho1;2 mutants were monitored at different times up to 7 days after sowing. Pictures were taken on day 7. Scale bar, 20 mm.

Pi (**Fig. 8C** and **Supplementary Fig. 4C**). These results indicate that both OsPHO1;1 and OsPHO1;2 are influx transporters for Pi driven by proton gradient rather than efflux transporters for Pi.

To confirm this result, we further expressed OsPHO1;2 in *Xenopus* oocytes. When the external pH was 5.5, oocytes expressing *OsPHO1;2* showed higher transport activity for Pi than those water-injected control (**Supplementary Fig. S5**). However, at pH 7.5 in the external solution, no transport activity of OsPHO1;2 for Pi was detected (**Supplementary Fig. S5**). These results further indicate that OsPHO1;2 is an H$^+$/Pi symporter.

Discussion

OsPHO1;1 and OsPHO1;2 are influx Pi transporters localized at the plasma membrane

Both *AtPHO1* in Arabidopsis and *OsPHO1;2* in rice are expressed in the root vascular cylinder and are involved in the root-to-shoot translocation of Pi based on the phenotype of knockout mutants (Poirier et al. 1991, Hamburger et al. 2002, Secco et al. 2010). These results implicate that AtPHO1 and OsPHO1;2 function as transporters for Pi; however, direct evidence for this is lacking. Expression of *AtPHO1* in yeast and *Xenopus* oocytes failed to detect the transport activity of AtPHO1 for Pi (Hamburger et al. 2002). Ectopic expression of *AtPHO1* in
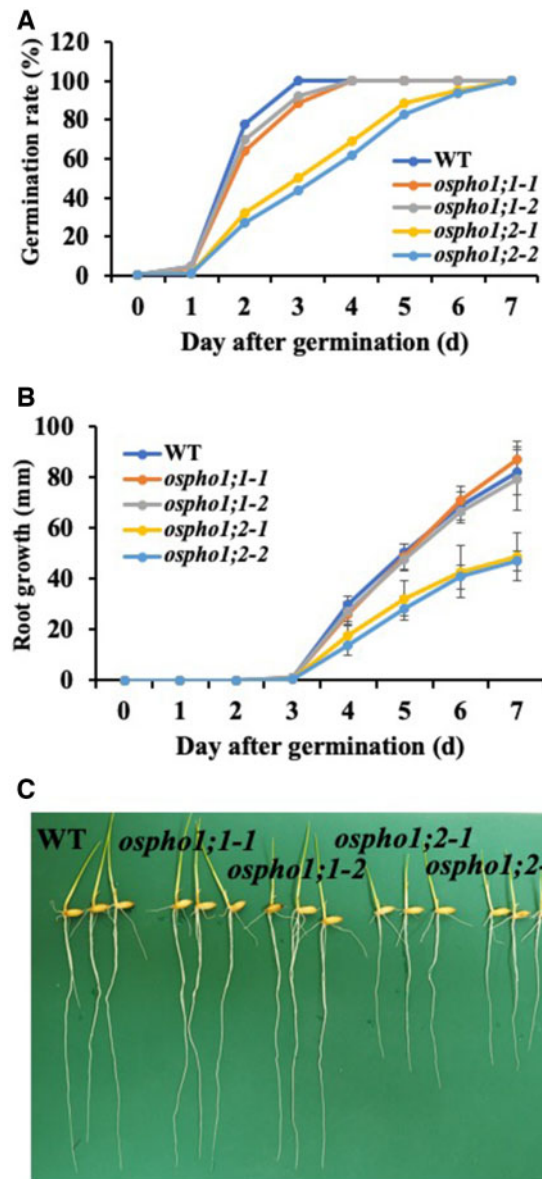
Arabidopsis and tobacco leaf cells resulted in Pi release to the extracellular medium (Arpat et al. 2012), implicating that AtPHO1 functions as an efflux transporter for Pi. The PHO1 homolog in animals was also characterized as a Pi efflux transporter (Giovannini et al. 2013). However, in the present study, we succeeded in directly detecting the transport activity of OsPHO1;1 and OsPHO1;2 for Pi both in a proteoliposome assay system and *Xenopus* oocytes (**Fig. 8**, Supplementary Figs. S4, S5). Furthermore, we found that both OsPHO1;1 and OsPHO1;2 are influx transporters for Pi driven by a H$^+$ gradient, but not efflux transporters for Pi (**Fig. 8**, Supplementary Figs. S4, S5). Since we investigated the transport activity in an heterologous system, the transport direction may differ in rice. However, this
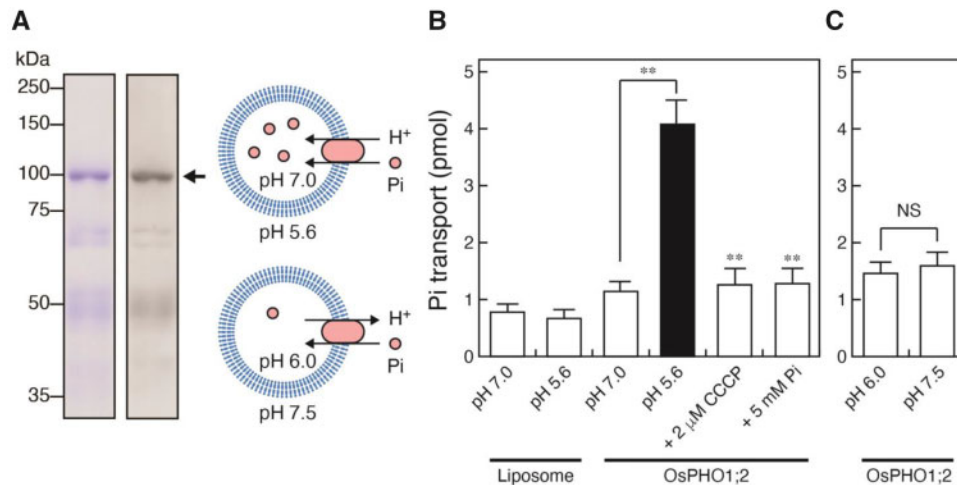
Fig. 8 Transport activity of OsPHO1;2 protein in the proteoliposome assay system. (A) Purification of OsPHO1;2. The purified fraction ($5\,\mu g$) was analyzed by SDS-PAGE and visualized by Coomassie Brilliant Blue staining (left) and by Western blot with anti-$6\times$His antibody (right). (B) Influx transport activity of OsPHO1;2 for ^{32}P. Proteoliposomes containing purified OsPHO1;2 or not were prepared in buffer at pH 7.0, incubated in buffer at either pH 7.0, pH 5.6 or pH 5.6 plus $2\,\mu M$ CCCP, and assayed after 2 min. *cis*-Inhibition of Pi transport was determined in the presence of the 5 mM non-labeled Pi. (C) Efflux transport activity of OsPHO1;2 for ^{32}P. Proteoliposomes containing purified OsPHO1;2 were prepared in buffer at pH 6.0, incubated in buffer at either pH 6.0 or pH 7.5, and assayed after 2 min. Data are means ($\pm$ SE) of technical replicates ($n = 3$–4). $P < 0.05$ (two-tailed paired Student's *t*-test). NS, not significant; CCCP, carbonyl cyanide *m*-chlorophenylhydrazone.

possibility seems unlikely based on the cell specificity of OsPHO1;1 localization at the phloem region of DVBs and of OsPHO1;2 at the xylem parenchyma cells of EVBs in node I (**Fig. 2A–D**), as discussed below.

We also found a difference in the subcellular localization of OsPHO1;1 and OsPHO1;2 compared with AtPHO1. When both OsPHO1;1 and OsPHO1;2 were expressed in rice leaf protoplast, they localized to the plasma membrane (**Supplementary Fig. S1E–L**), which is agreement with their roles as Pi transporters. However, AtPHO1 in Arabidopsis was reported to be largely localized to the Golgi and *trans*-Golgi network under normal Pi status (Arpat et al. 2012), although it seems that partial protein was relocated to the plasma membrane in leaves infiltrated with a high P solution (Arpat et al. 2012). There are two explanations for this result; one is that only a minor fraction of AtPHO1 localized to the plasma membrane is responsible for Pi export and the other one is that AtPHO1 first mediates Pi into the endosomes, followed by the release of Pi export to the extracellular space via exocytosis and rapid recycling of AtPHO1 away from the plasma membrane (Arpat et al. 2012). However, given the fact that the inhibition of root-to-shoot translocation of Pi was also observed under normal P conditions and that P concentration in soil solution is usually very low ($< 10\,\mu M$) (Hamburger et al. 2002, Secco et al. 2010, Lambers and Plaxton 2015), localization at the plasma membrane fits the role of AtPHO1 in the root-to-shoot translocation of Pi.

The exact reasons for the difference in transport direction (influx vs. efflux) and subcellular localization (plasma membrane vs. Golgi and *trans*-Golgi network) in AtPHO1 in Arabidopsis and in OsPHO1;1 and OsPHO1;2 in rice is unknown. AtPHO1, OsPHO1;1 and OsPHO1;2 share about 50% identity (Secco et al. 2010). AtPHO1 proteins contain two distinct domains, the SPX domain (named after proteins SYG1/ PHO81/XPR1) in the amino-termini and a carboxyl (C)-terminal domain (Secco et al. 2012). Based on the predicted membrane topologies (**http://aramemnon.botanik.uni-koeln.de/**), the C-terminal domain contains the first four transmembrane α-helices (4TM) and the following hydrophobic region harboring the EXS domain (named after ERD1, XPR1 and SYG1) (Wege et al. 2016). The EXS domain in the C-termini is sufficient for the correct subcellular localization of AtPHO1 to the Golgi and *trans*-Golgi network. The EXS domain is also essential for the Pi export activity although by itself cannot mediate Pi export (Wege et al. 2016). The 4TM of AtPHO1 in Arabidopsis and OsPHO1;1 and OsPHO1;2 in rice showed high consensus, while the EXS domain showed low consensus (Secco et al. 2012), which may account for the difference in the subcellular localization and transport direction. However, the exact mechanism for these differences remains to be investigated.

OsPHO1;1 and OsPHO1;2 are involved in intervascular transfer of Pi in node I

Previous studies focused on the role of *OsPHO1;2* expressed in the roots of rice (Secco et al. 2010, Jabnoune et al. 2013); however, in the present study, we found that both *OsPHO1;1* and *OsPHO1;2* are also highly expressed in node I at the reproductive stage, and that they play an important role in the intervascular transfer of Pi, which is required for the allocation of Pi to the seed. The distribution of mineral elements to the seed in node I includes several steps such as unloading of a mineral nutrient from xylem flow in EVB, transfer through symplast or apoplast of parenchyma cell bridge (PCB) and reloading to xylem or phloem of DVB (Yamaji and Ma 2014, Yamaji and Ma 2017). *OsPHO1;1* is mainly expressed in the phloem region of DVBs, while *OsPHO1;2* is expressed in the xylem parenchyma cells including xylem transfer cells of EVBs (**Fig. 2A–D**). Therefore,
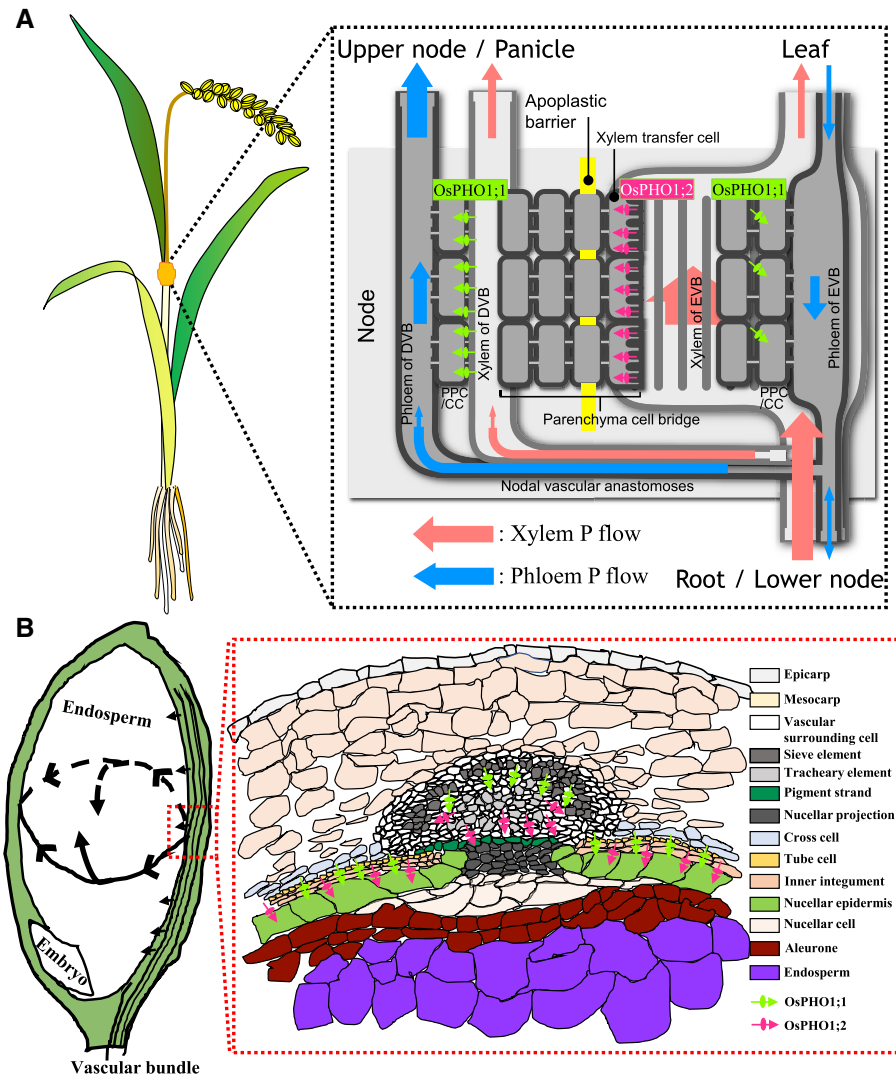
Fig. 9 Schematic presentation of the roles of OsPHO1;1 and OsPHO1;2 in the allocation of P to seeds in rice. (A) Role of OsPHO1;1 and OsPHO1;2 in the intervascular transfer of P in node I. Unloading of P from the xylem of the EVBs in node I is mediated by OsPHO1;2 and further loading of P to the phloem of the DVBs by OsPHO1;1. (B) Role of OsPHO1;1 and OsPHO1;2 in the delivering of P from the maternal tissues to the filial tissues. OsPHO1;1 and OsPHO1;2 localized in the ovular vascular trace mediate the unloading of P passing through node I. OsPHO1;1 localized in the outer layer of the inner integument and OsPHO1;2 localized in the nucellar epidermis mediate the final step of P transfer from the maternal tissues to the filial tissues. Arrows indicate the direction of P transport.

OsPHO1;2 is responsible for unloading Pi from the xylem of EVBs in node I (**Fig. 9A**). This is consistent with findings that OsPHO1;2 functions as an influx transporter of Pi and that knockout of this gene resulted in an increased distribution of Pi to the flag leaf but decreased P distribution to the grain (**Figs. 5D, 6**). This role of OsPHO1;2 is similar to that of SPDT, but the contribution of OsPHO1;2 is much larger than that of SPDT based on the phenotype of mutants. Knockout of *SPDT* reduced 20% P in the seeds (Yamaji et al. 2017), while knockout of *OsPHO1;2* resulted in 50–56% decrease in P in the seeds (**Fig. 5B**). As a result, knockout of *OsPHO1;2* significantly decreased seed size (**Fig. 4G**), while knockout of *SPDT* did not affect seed size under normal P condition (Yamaji et al. 2017).

On the other hand, OsPHO1;1 is involved in reloading Pi to the phloem of DVBs (**Fig. 9A**). Knockout of *OsPHO1;1* also decreased P distribution to the grain, but to a less extent

compared with *OsPHO1;2* knockout (**Fig. 5C, D**). Other unidentified transporters may be involved in this process, and/or contribution of the symplastic transport pathway from EVBs to DVBs through the PCB is larger.

OsPHO1;1 and OsPHO1;2 expressed in the caryopsis are required for loading Pi to the seed

We occasionally found that *OsPHO1;1* and *OsPHO1;2* are also expressed in the caryopsis (**Fig. 3**). Mineral elements passing through node I are finally unloaded into the seed from OVT, the point of entry into the grain (Krishnan and Dayanandan 2003, Wu et al. 2016). The OVT contains both phloem and xylem cells. Both *OsPHO1;1* and *OsPHO1;2* are expressed in the OVT (**Fig. 3**), implicating their role in delivering P from the maternal tissues to the filial tissues (the aleurone and endosperm) (**Fig. 9B**). This is supported by the fact that the *ospho1;2*

mutant showed a higher P concentration in the husk, although it was not observed in the *ospho1;1* mutant (**Fig. 5A, B**). In addition, *OsPHO1;1* and *OsPHO1;2* were expressed in the outer layer of the inner integument and in the nucellar epidermis, respectively (**Fig. 3**). The single layer of integument and the nucellar epidermis are separated by a cuticular layer, and there are no plasmodesmata between these two layers (**Krishnan and Dayanandan 2003**). OsPHO1;1 and OsPHO1;2 are probably involved in the final step of P transfer from the maternal tissues to the filial tissues (**Fig. 9B**), although the detailed mechanisms require further investigation. Recently, it was reported that *AtPHO1* in Arabidopsis was also expressed in the chalazal seed coat of developing seeds (**Vogiatzaki et al. 2017**). This specific expression is crucial for mediating P transfer from the seed coat to the embryo at the mature green stage (**Vogiatzaki et al. 2017**).

In conclusion, our results present a novel role for *OsPHO1;1* and *OsPHO1;2* in the allocation of Pi to seeds at the reproductive stage of rice (**Fig. 9**). Both OsPHO1;1 and OsPHO1;2 are plasma membrane-localized proteins and showed influx transport activities for Pi. *OsPHO1;1* and *OsPHO1;2* expressed in node I are involved in the intervascular transfer of P, through unloading of P from the xylem of the EVBs by OsPHO1;2 and further loading of P to the phloem of the DVBs by OsPHO1;1 (Fig. 9A). Furthermore, *OsPHO1;1* and *OsPHO1;2* expressed in the caryopsis are also involved in the delivery of P from the maternal tissues to the filial tissues (Fig. 9B). These roles of *OsPHO1;1* and *OsPHO1;2* are important for seed development and subsequently seed germination and early plant growth in rice.

Materials and Methods

Expression patterns of *OsPHO1;1* and *OsPHO1;2*

To investigate the expression patterns of *OsPHO1;1* and *OsPHO1;2*, rice (cv. Nipponbare) was grown in a paddy field and various tissues were sampled at the grain-filling stage. Total RNA was extracted using an RNeasy Plant Mini Kit (Qiagen, https://www.qiagen.com), and cDNAs were synthesized by ReverTra Ace qPCR RT Master Mix with gDNA Remover (TOYOBO, https://www.toyobo.co.jp/). Subsequently, cDNAs were amplified by Sso Fast EvaGreen Supermix (Bio-Rad, https://www.bio-rad.com/) and quantitative real-time PCR was performed on CFX384 (Bio-Rad). *Histone H3* (Os06g0130900) was used as an internal standard. Relative expression levels were calculated by the comparative Ct method. Three independent biological replicates were made for each treatment.

Furthermore, node I was separated by LMD (Applied Biosystems Arcturus Laser Capture Microdissection System, https://www.thermofisher.com/) into EVBs (phloem and xylem regions) and DVBs. Node I was sampled from rice grown in soil at the milky stage and fixed in a solution containing ethanol/acetic acid at a ratio of 3:1. Other procedures were the same as described previously (**Takahashi et al. 2010**, **Song et al. 2014**). Total RNA of each tissue isolated was extracted using a PicoPure RNA Isolation Kit (Applied Biosystems, https://www.thermofisher.com/jp/ja/home/brands/applied-biosystems.html) followed by DNase I (Qiagen) treatment and was then converted into cDNA using SuperScript III (Invitrogen, https://www.thermofisher.com/jp/ja/home/brands/invitrogen.html). The primer sequences used for investigating gene expression are shown in **Supplementary Table S1**.

Subcellular localization of *OsPHO1;1* and *OsPHO1;2*

To investigate the subcellular localization of OsPHO1;1 and OsPHO1;2, we constructed a translational OsPHO1;1-GFP and GFP-OsPHO1;2 fusion. The ORF of *OsPHO1;1* without the stop codon and the ORF of *OsPHO1;2* with the stop codon were amplified by PCR from rice (cv Nipponbare) node cDNA for OsPHO1;1-GFP and GFP-OsPHO1;2 fusion, respectively. Then, it was subcloned into the binary vector pGWB5 or pGWB6 (**Nakagawa et al. 2007**). Rice protoplasts were prepared from leaves of 2-week-old seedlings grown hydroponically and were used for transformation by the polyethylene glycol method as described previously (**Chen et al. 2006**). GFP fluorescence was observed under a confocal laser scanning microscope (TCS SP8x, https://www.leica-microsystems.com/). The primer sequences used for amplifying the ORF of *OsPHO1;1* and *OsPHO1;2* for subcellular localization are shown in **Supplementary Table S1**.

Tissue specificity and cell specificity of *OsPHO1;1* and *OsPHO1;2* expression

To examine the tissue-specific expression of *OsPHO1;1* and *OsPHO1;2*, we generated transgenic rice lines carrying *OsPHO1;1* or *OsPHO1;2* promoter fused with GFP. The promoter region of *OsPHO1;1* (2.0 kb) or *OsPHO1;2* (2.0 kb) was amplified from rice genomic DNA by PCR using the primers listed in **Supplementary Table S1**. Then, the fragment amplified was fused to the GFP fragment isolated from a pBluescript vector (Agilent, **http://www.genomics.agilent.com/**). The fused DNA was inserted into the pPZP2H-lac vector (**Fuse et al. 2001**). The derived construct was transformed into calluses (cv. Nipponbare) by *Agrobacterium*-mediated transformation (**Hiei et al. 1994**). Immunostaining with an anti-GFP antibody (https://www.thermofisher.com/antibody/product/GFP-Antibody-Polyclonal/A-11122) was performed in node I and caryopsis of the T1 generation of the transgenic rice and non-transgenic rice as a negative control as described before (**Yamaji and Ma 2007**). Node I was sampled from rice grown in soil at the grain-filling stage, and the caryopsis was prepared by dehusking the grain at days 6 after pollination.

Phenotypic analysis of mutant lines

Two retrotransposon *Tos17* insertion mutants of *OsPHO1;1* (NF1695/*ospho1;1–1* and NG0988/*ospho1;1–2*), two retrotransposon *Tos17* insertion mutants of *OsPHO1;2* (NC0015/*ospho1;2–1* and NE2044/*ospho1;2–2*) and WT rice (*O. sativa* L., cv. Nipponbare) were obtained from the rice genome resource center. Twenty-four-day-old seedlings of WT rice and mutants pre-cultured hydroponically were transplanted to the experimental paddy field of Okayama University on June 21 and harvested on October 8, 2018. At harvest, plant height, tiller number, fertility, grain number per panicle and 1,000-grain weight were investigated. Twenty-four biological replicates (three plots with eight replicates each) were made for each line. At the ripening stage, plants were separated into brown rice, husk, rachis, peduncle, nodes I and II, flag leaf blade, flag leaf sheath, leaf II blade, leaf II sheath, internode II and others. The concentration of mineral elements was determined in each organ as described below. The percentage distribution of P in different organs was calculated as P content in each organ/total P content $\times$ 100.

Determination of mineral elements

All samples were dried in an oven at 70°C for at least 3 d. Then, the dried samples were digested with concentrated HNO_3 (60%) at a temperature of up to 135°C. The concentration of mineral elements in the digested solution was determined by inductively coupled plasma mass spectrometry (7700X; Agilent Technologies, https://www.agilent.com/).

Short-term stem-feeding experiments with radio-isotope ^{32}P

For the stem-feeding experiment, WT rice and *ospho1;1/ospho1;2* mutants were grown in the paddy field. At the filling stage, the upper part was cut at internode III below node II and placed in a nutrient solution containing ^{32}P (4 MBq 400 ml^{-1}; 10 pM) with 1 μM cold Pi. After 24-h feeding from the cut end, different organs including flag leaf, node I and panicle were sampled and immediately subjected to radioactivity measurement with a liquid scintillation analyzer (PerkinElmer, https://www.perkinelmer.com) without liquid scintillator (Cerenkov radiation mode). P distribution to different organs was calculated based on the radioactivity of each part. Four independent biological replicates were made for each line.

Germination and early growth of the WT rice and mutants

To investigate seed germination and early growth, we soaked 100 seeds each of WT rice and two mutants in water at 30°C in the dark for 2 d and then transferred to a net floating on a 0.5 mM CaCl$_2$ solution. The root growth and germination rates were monitored at different times up to 7 d.

Transport activity assay

For transport activity assay by proteoliposomes, the expression, purification and reconstitution of OsPHO1;1 and OsPHO1;2 were carried out as described previously (Miyaji et al. 2015). Aliquots (25 μg) of purified OsPHO1;1 or OsPHO1;2 were mixed with liposomes (500 μg) and frozen at −80°C for at least 10 min. The mixture was diluted 100-fold with reconstitution buffer containing 20 mM MOPS-Tris (pH 7.0) for influx experiment or MES-Tris (pH 6.0) for efflux experiment, 0.1 M potassium acetate and 5 mM magnesium acetate. Reconstituted proteoliposomes were pelleted by centrifugation at 200,000 × *g* for 1 h at 4°C and then suspended in reconstitution buffer (0.2 ml). Asolectin liposomes were prepared as described previously (Miyaji et al. 2015). Western blot was performed as described previously (Miyaji et al. 2015). Transport assays were carried out by the gel permeation procedure as described previously (Miyaji et al. 2015). For influx experiment, reaction mixtures (130 μl) containing 0.3 μg of protein were incorporated into proteoliposomes, 40 mM MES-Tris (pH 5.6) or 20 mM MOPS-Tris (pH 7.0), 0.1 M potassium acetate, 5 mM magnesium acetate, 10 mM KCl and 100 μM [^{32}P] KH$_2$PO$_4$ (3.7 MBq μmol^{-1}; PerkinElmer). In the case of H$^+$/Pi antiport (efflux), reaction mixtures (130 μl) containing 0.3 μg of protein were incorporated into proteoliposomes, 20 mM MOPS-Tris (pH 7.5) or 20 mM MES-Tris (pH 6.0), 0.1 M potassium acetate, 5 mM magnesium acetate, 10 mM KCl and 100 μM [^{32}P] KH$_2$PO$_4$ (3.7 MBq μmol^{-1}; PerkinElmer).

Oocytes for Pi transport activity assay were isolated from *Xenopus laevis*. Procedures for defolliculation, culture conditions and selection were as described previously (Ma et al. 2006). The ORF of *OsPHO1;2* was amplified by PCR. The ORF was cloned into the *Bgl*II site of a *Xenopus* oocyte expression vector, pXβG-ev1 (Preston et al. 1992). Capped RNA was then synthesized from a linearized pXβG-ev1 plasmid (cut by *Xba*I enzyme) by in vitro transcription with an mMASSAGE mMACHINE high-yield capped RNA transcription kit (Ambion, https://www.thermofisher.com/jp/ja/home/brands/invitrogen/ambion.html), according to the manufacturer's instructions. A volume of 50 nl (1 ng nl^{-1}) cRNA was injected into the oocytes using a Nanoject II automatic injector (Drummond Scientific, https://www.drummondsci.com/). As a negative control, 50 nl of RNase-free water was injected. After incubation in MBS at 18°C for 1 d, 5–7 oocytes were incubated with 500 μl of MBS without Ca (MBS-Ca) containing 1 μl of [^{32}P]H$_3$PO$_4$ (37 MBq ml^{-1}) and 0.1 mM NaH$_2$PO$_4$ at pH 5.5 in 10 mM MES buffer or pH 7.5 in Tris-HCl buffer. After 30 min incubation at 18°C, the oocytes were washed in ice-cold MBS five times and, then, the radioactivity in the oocytes was measured with a scintillation analyzer (PerkinElmer). Four independent biological replicates were made for each treatment. The primer sequences used for amplifying the ORF of *OsPHO1;1* and *OsPHO1;2* for transport activity analysis are shown in **Supplementary Table S1**.

Statistical analysis

Tukey's test, Duncan's test and Student's *t*-test were applied to test differences among treatments at $P < 0.05$ or $P < 0.01$.

Supplementary Data

Supplementary data are available at PCP online.

Acknowledgments

We thank Prof. N. Nelson (Tel Aviv University) for providing the bacterial expression vector.

Disclosures

The authors have no conflicts of interest to declare.

References

Arpat, A.B., Magliano, P., Wege, S., Rouached, H., Stefanovic, A. and Poirier, Y. (2012) Functional expression of PHO1 to the Golgi and *trans*-Golgi network and its role in export of inorganic phosphate. *Plant J.* 71: 479–491.

Chang, M.X., Gu, M., Xia, Y.W., Dai, X.L., Dai, C.R., Zhang, J., et al. (2019) OsPHT1;3 mediates uptake, translocation, and remobilization of phosphate under extremely low phosphate regimes. *Plant Physiol.* 179: 656–670.

Chen, S., Tao, L., Zeng, L., Vega-Sanchez, M.E., Umemura, K. and Wang, G.L. (2006) A highly efficient transient protoplast system for analyzing defence gene expression and protein-protein interactions in rice. *Mol. Plant Pathol.* 7: 417–427.

Fuse, T., Sasaki, T. and Yano, M. (2001) Ti-plasmid vectors useful for functional analysis of rice genes. *Plant Biotechnol.* 18: 219–222.

Giovannini, D., Touhami, J., Charnet, P., Sitbon, M. and Battini, J.L. (2013) Inorganic phosphate export by the retrovirus receptor XPR1 in metazoans. *Cell Rep.* 3: 1866–1873.

Hamburger, D., Rezzonico, E., MacDonald-Comber Petetot, J., Somerville, C. and Poirier, Y. (2002) Identification and characterization of the Arabidopsis *PHO1* gene involved in phosphate loading to the xylem. *Plant Cell* 14: 889–902.

Hiei, Y., Ohta, S., Komari, T. and Kumashiro, T. (1994) Efficient transformation of rice (*Oryza sativa* L.) mediated by *Agrobacterium* and sequence analysis of the boundaries of the T-DNA. *Plant J.* 6: 271–282.

Jabnoune, M., Secco, D., Lecampion, C., Robaglia, C., Shu, Q. and Poirier, Y. (2013) A rice *cis*-natural antisense RNA acts as a translational enhancer for its cognate mRNA and contributes to phosphate homeostasis and plant fitness. *Plant Cell* 25: 4166–4182.

Krishnan, S. and Dayanandan, P. (2003) Structural and histochemical studies on grain-filling in the caryopsis of rice (*Oryza sativa* L.). *J. Biosci.* 28: 455–469.

Lambers, H. and Plaxton, W.C. (2015) Phosphorus: back to the roots. *Annu. Plant Rev.* 48: 3–22.

Lott, J.N., Bojarski, M., Kolasa, J., Batten, G.D., Campbell, L.C., Amigó, J.M., et al. (2009) A review of the phosphorus content of dry cereal and legume crops of the world. *Int. J. Agric. Resour. Gov. Ecol.* 8: 351–370.

Ma, J.F., Tamai, K., Yamaji, N., Mitani, N., Konishi, S., Katsuhara, M., et al. (2006) A silicon transporter in rice. *Nature* 440: 688–691.

Miyaji, T., Kuromori, T., Takeuchi, Y., Yamaji, N., Yokosho, K., Shimazawa, A., et al. (2015) AtPHT4;4 is a chloroplast-localized ascorbate transporter in *Arabidopsis*. *Nat. Commun.* 6: 5928.

Nakagawa, T., Kurose, T., Hino, T., Tanaka, K., Kawamukai, M., Niwa, Y., et al. (2007) Development of series of gateway binary vectors, pGWBs, for realizing efficient construction of fusion genes for plant transformation. *J. Biosci. Bioeng.* 104: 34–41.

Pariasca-Tanaka, J., Vandamme, E., Mori, A., Segda, Z., Saito, K., Rose, T.J., et al. (2015) Does reducing seed-P concentrations affect seedling vigor and grain yield of rice? *Plant Soil* 392: 253–266.

Poirier, Y., Thoma, S., Somerville, C. and Schiefelbein, J. (1991) A mutant of *Arabidopsis* deficient in xylem loading of phosphate. *Plant Physiol.* 97: 1087–1093.

Preston, G.M., Carroll, T.P., Guggino, W.B. and Agre, P. (1992) Appearance of water channels in *Xenopus* oocytes expressing red cell CHIP28 protein. *Science* 256: 385–387.

Raboy, V. (2001) Seeds for a better future: 'low phytate', grains help to overcome malnutrition and reduce pollution. *Trends Plant Sci.* 6: 458–462.

Raboy, V. (2009) Approaches and challenges to engineering seed phytate and total phosphorus. *Plant Sci.* 177: 281–296.

Sasaki, A., Yamaji, N., Mitani-Ueno, N., Kashino, M. and Ma, J.F. (2015) A node-localized transporter OsZIP3 is responsible for the preferential distribution of Zn to developing tissues in rice. *Plant J.* 84: 374–384.

Secco, D., Baumann, A. and Poirier, Y. (2010) Characterization of the rice *PHO1* gene family reveals a key role for *OsPHO1;2* in phosphate homeostasis and the evolution of a distinct clade in dicotyledons. *Plant Physiol.* 152: 1693–1704.

Secco, D., Wang, C., Arpat, B.A., Wang, Z., Poirier, Y., Tyerman, S.D., et al. (2012) The emerging importance of the SPX domain-containing proteins in phosphate homeostasis. *New Phytol.* 193: 842–851.

Song, W.Y., Yamaki, T., Yamaji, N., Ko, D., Jung, K.H., Fujii-Kashino, M., et al. (2014) A rice ABC transporter, OsABCC1, reduces arsenic accumulation in the grain. *Proc. Natl. Acad. Sci. USA* 111: 15699–15704.

Takahashi, H., Kamakura, H., Sato, Y., Shiono, K., Abiko, T., Tsutsumi, N., et al. (2010) A method for obtaining high quality RNA from paraffin sections of plant tissues by laser microdissection. *J. Plant Res.* 123: 807–813.

Vogiatzaki, E., Baroux, C., Jung, J.Y. and Poirier, Y. (2017) PHO1 exports phosphate from the chalazal seed coat to the embryo in developing *Arabidopsis* seeds. *Curr. Biol.* 27: 2893–2900.

Wege, S., Khan, G.A., Jung, J.Y., Vogiatzaki, E., Pradervand, S., Aller, I., et al. (2016) The EXS domain of PHO1 participates in the response of shoots to phosphate deficiency via a root-to-shoot signal. *Plant Physiol.* 170: 385–400.

White, P.J. and Veneklaas, E.J. (2012) Nature and nurture: the importance of seed phosphorus content. *Plant Soil* 357: 1–8.

Wu, X., Liu, J., Li, D. and Liu, C.M. (2016) Rice caryopsis development I: Dynamic changes in different cell layers. *J. Integr. Plant Biol.* 58: 772–785.

Yamaji, N. and Ma, J.F. (2007) Spatial distribution and temporal variation of the rice silicon transporter Lsi1. *Plant Physiol.* 143: 1306–1313.

Yamaji, N. and Ma, J.F. (2009) A transporter at the node responsible for intervascular transfer of silicon in rice. *Plant Cell* 21: 2878–2883.

Yamaji, N. and Ma, J.F. (2014) The node, a hub for mineral nutrient distribution in graminaceous plants. *Trends Plant Sci.* 19: 556–563.

Yamaji, N. and Ma, J.F. (2017) Node-controlled allocation of mineral elements in Poaceae. *Curr. Opin. Plant Biol.* 39: 18–24.

Yamaji, N., Mitatni, N. and Ma, J.F. (2008) A transporter regulating silicon distribution in rice shoots. *Plant Cell* 20: 1381–1389.

Yamaji, N., Sakurai, G., Mitani-Ueno, N. and Ma, J.F. (2015) Orchestration of three transporters and distinct vascular structures in node for intervascular transfer of silicon in rice. *Proc. Natl. Acad. Sci. USA* 112: 11401–11406.

Yamaji, N., Sasaki, A., Xia, J.X., Yokosho, K. and Ma, J.F. (2013a) A node-based switch for preferential distribution of manganese in rice. *Nat. Commun.* 4: 2442.

Yamaji, N., Takemoto, Y., Miyaji, T., Mitani-Ueno, N., Yoshida, K.T. and Ma, J.F. (2017) Reducing phosphorus accumulation in rice grains with an impaired transporter in the node. *Nature* 541: 92–95.

Yamaji, N., Xia, J.X., Mitani-Ueno, N., Yokosho, K. and Ma, J.F. (2013b) Preferential delivery of zinc to developing tissues in rice is mediated by P-type heavy metal ATPase OsHMA2. *Plant Physiol.* 162: 927–939.

Zhao, P.F., You, Q.Y. and Lei, M.G. (2019) A CRISPR/Cas9 deletion into the phosphate transporter SlPHO1;1 reveals its role in phosphate nutrition of tomato seedlings. *Physiol. Plant.* 167: 556–563.